Unaccounted for uncertainties in radioaerosol assays as used in plume reconstruction or treaty verification

Robert B. Hayes
North Carolina State University, College of Engineering
Nuclear Engineering Department
Retrospective Dosimetry and Nuclear Assay
2500 Stinson Dr. Raleigh, NC 27695-7909, USA
E-mail: rbhayes@ncsu.edu

Abstract:

The typical approach used in air sampling is to ascribe the radiological concentration of interest in an air sample to the ratio of filter activity to volume pulled. This attribution is reasonable provided the sample is representative, however, the uncertainties ascribed to this concentration are generally considered Poisson errors from the counting scheme used. This work will show how the actual dispersion can be one or two orders of magnitude larger in some cases even when the radioaerosol has constant specific activity due to the lognormal size distribution of the particulate sampled. Applications in plume monitoring and the actual release from the February 2014 event at the Waste Isolation Pilot Plant in New Mexico USA will be considered and presented.

Keywords: air monitoring; uncertainty; dispersion; sampling

1. Introduction

Air sampling is one of the key aspects to the comprehensive test ban treaty (CTBT) monitoring regime. Samples of interest include radioaersols (e.g., radioiodines and transuranics) along with noble gases (eg. Xe isotopes). This work addresses only the aerosol physics of this sampling but as such, it also has applicability to operational health physics and radiological emergency response. The application to the February 2014 transuranic waste drum deflagration at the Waste Isolation Pilot Plant (WIPP) in southeast New Mexico USA will be evaluated as a case in point on the effect described here [1]. The effects of aerosol physics on the sample collection will demonstrate how typical air sampling interpretations for common assays will underestimate true dispersion by as much as an order of magnitude in most cases, possibly even 2 orders.

1.1 Aerosol sampling and assay

The process for taking an air sample has largely been unchanged for the past 70 years. This method involves pulling a known volume of air through a filter and then assaying that filter. The sampled air is then ascribed a concentration value equal to the ratio of the filter assay activity to the volume of air pulled.

Typically, the volume of air is known quite precisely and the assay is constrained to Poisson statistics relegating the dominant uncertainty in the airborne concentration estimate to that of the Poisson counting in the assay.

1.2 Representative sampling

In order to obtain a quality sample, the collection of all particulate must be representative of the total population present in the space of interest. This is typically only considered to be an issue when the sampling is taking place in a duct or exhaust system. When sampling an effluent, the linear face velocity through the filter has to be equal to that of the general volume surrounding it to prevent over or under sampling of the particulate. This can be challenging when the linear flow rates of the effluent vary or are turbulent.

Undersampling is expected to occur when the linear face velocity through the filter is lower than the bulk volume around the sampling head. This will cause some of the smaller particulate to follow the flow path avoiding the filter even though it would have initially traversed it were the sampling head not present.

Oversampling is expected when the linear face velocity through the filter is higher than the bulk volume around the sampling head. This would cause particulate which otherwise would not have passed along the intake face of the filter to divert from its ambient path into the filter due to the higher sampling flow rate.

One way to overcome this challenge for dynamic flow conditions is to use a shrouded probe as shown in Figure 1 [2]. The shroud forces air through the outer channel to take a more linear path surrounding the filter's sample head and therefore can prevent any under- or oversampling.

1.3 Aerosol physics

Aerosols evolve in an effectively fractal manner. They are not generally spherical but rather dendritic and are composed primarily of organic matter, micron-sized silicates and/or ocean mist near the coast [3]. Their evolution will depend on relative humidity, particle density and types.

Typical binding forces are those of Van der Waals when gross kinetic impact of any kind occurs. Aerosol particulate growth is not spherical but erratic resulting in dynamic

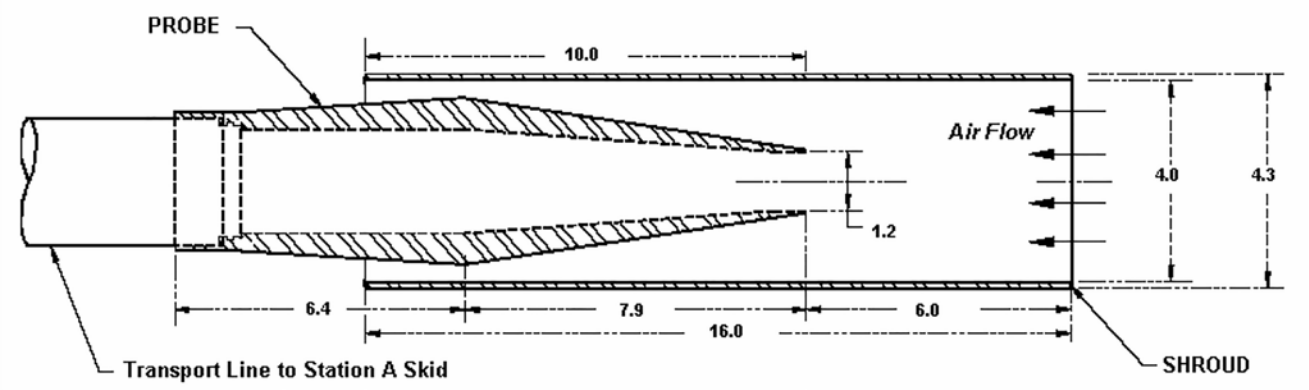

Figure 1: Shrouded probe schematic show from a cross sectional view. [2]

properties such as changing density, heat capacity and obviously aerodynamic radii. Reviews of the intricacies of these dynamic dependencies can be found elsewhere [4, 5].

1.3.1 Radioaerosol physics

Radioaerosols in particular can be extremely erratic in their evolution when they decay through charged particle emission. When a gaseous radionuclide (such as radon or its progeny) decays through charged particle emission, the resulting heavy metal gas has a charge that will induce a polarization in all nearby aerosols. The resultant dipoles in the vicinity of a point charge will result in an attractive potential to pull the radionuclide into a bound state with one or more ambient aerosols.

This additional Coulomb-based potential in radioaerosol physics only further exacerbates the evolutionary growth properties in any given species. The radical electric potential shift which can occur when spontaneous charge generation is placed on the aerosol or gas (from charged particle emission in radioactive decay) allows for rapid growth and is unique to the radioactive decay process (including recoil effects from decay such as dislodging).

A radioactive aerosol can begin as an inert isolated gaseous species such as radon, radon progeny or radioiodines. With radioiodines, these can combine with atmospheric water or other materials to become an aerosol. Radon progeny can remain as a gas through its decay series or combine with ambient aerosols to become part of the bound fraction of the progeny (conversely, that part which does not combine with any aerosols is simply the unbound fraction). These fractions are expected to depend on relative abundances of the radionuclide and ambient aerosols along with temperature, relative humidity etc.

1.3.2 Sampling physics

The action of sampling a gas or aerosol for assay requires either measurement in some in-situ fashion (generally resulting in dismal sensitivity with low concentrations) or concentrating it in some medium for characterization. With an aerosol, this is done by pulling air through a filter such that the filter concentrates the particulate within its volume. Gaseous species are typically collected by pulling air through zeolite or activated charcoal to later be boiled off in a vacuum and then concentrated for assay.

With the air filter, there are 4 main mechanisms for fixing the analyte in the medium. These are inertial impaction (similar to a projectile into mud), interception (particles too massive to fit through the pores), diffusion (Van der-Waals adhesion) and electrostatic attraction (requiring a net charge, although not seen in Figure 2, see section 1.3.1).

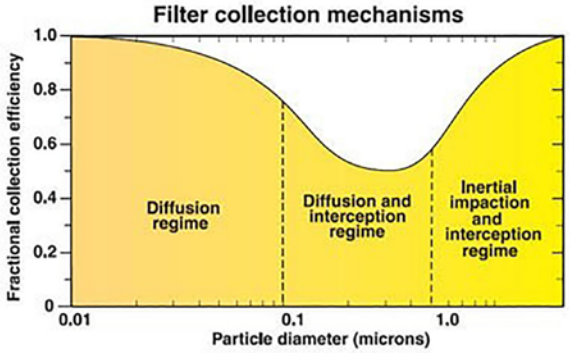

Figure 2: Filter collection mechanisms labelling dominant sampling efficiencies grouped by particle size. Note the abscissa is given in logarithmic scale. [3]

As a result of the variety of physics taking place when sampling an aerosol, the particle size collection efficiency is dependent on a number of factors (including flow rate, filter characteristics etc.). As a generalization, the particle size efficiency shown in Figure 2 can be used as a reasonable approximation to typical behaviours. Here, dominant sampling mechanism regimes are shown as a function of aerosol size.

It is significant to note that in the respirable range (when particulate is able to make it all the way down into the lung alveoli and be retained for a dose intake) is exactly where the filter efficiency is both lowest and has the largest changes (0.1 to 5 μm). This uncertainty in filter efficiency for the respirable range contributes to the reason why dose should not be ascribed to individuals based only on

air monitoring data [6] compared to the far more reliable and standard bioassay in determining actual radionuclide intake. This is one important contribution to dispersion in aerosol monitoring which is independent of the final filter assay but there are others.

2. Plume monitoring

With the advent of any nuclear detonation, leakage of the gaseous constituents from the event will then pour into the environment creating a plume. The simplest propagation model for plume evolution is probably Gaussian diffusion with advective transport. This means that as the material follows airflow, it will diffuse in all directions driven by simple Fickian mechanics. Atmospheric stratification along with ground boundaries complicate the transport along with any convective or turbulent flows.

To the extent that the plume propagation can be accurately predicted, multiple sample points would then enable characterization of the same. Two or three points are likely inadequate to fully characterize any plume unless the source term itself was already well known in time and space. Backtracking a potential plume around the globe can quickly become intractable without source term knowledge or real time monitoring of the plume itself [6].

2.1 Footprint characterization

If a known release had occurred, sampling teams would generally prefer to stay on the penumbra of the fallout footprint caused by the plume passage and deposition. This prevents the sampling teams from being required to don personal protective equipment (PPE) and so prevent skin contamination. Further, vehicle contamination would also occur if sampling missions were not constrained to the outskirts of the fallout. Any vehicle and personnel radioactivity accumulation would create the need for decontamination and so full hotline support to eventually doff the PPE and reuse of the vehicle. These activities would necessitate additional manpower and resources for decontamination rather than sampling, assessment and control.

2.1.1 Low concentration sample drivers

Due to these inhibitions from sampling in contaminated areas, only those areas that have barely detectable levels of the radionuclides of interest may be measured so that PPE is not required. Higher levels of the plume footprint are then characterized from the air using large arrays of NaI logs for gamma detection [7]. This means that air and soil samples taken from ground teams are invariably acquired from those regions of low or very low contamination.

The same result (expected low activity) is generally realized for routine air samples, even those taken from an effluent stack. This is because facility release limits are generally sufficiently low that the maximum possible public or environmental dose consequence is a small fraction of normal background dose. In order to comply with facility limits, effluent content of any controlled radionuclides have to be low. In many cases, the dominant transuranic (TRU) release content is from resuspended fallout created by atmospheric weapons testing in the past century [8]. The purpose for most air samples is to prove that no release did occur so again, overwhelmingly, air samples for controlled radionuclides have low to very low anthropogenic radionuclide content.

2.2 WIPP event

On February 14 of 2014, a deflagration took place in a TRU drum sent to the WIPP for permanent disposal by the Los Alamos National Laboratory. The WIPP facility itself is a deep salt mine and the radiation monitoring system detected the breach shifting the effluent airflow to a suite of high efficiency particulate air (HEPA) filters preventing a large environmental release. The system had a small leak due to industrial bypass filters designed for mining operations to divert the airflow which were not rated for nuclear operations (they were designed and built in the 1980's prior to modern nuclear standards for geological repository ventilation systems). The event took place while the regulatory compliant radiation monitoring system was functioning including on and offsite air sampling stations.

The resultant plume (along with offsite sampling stations labelled as pink flags) is shown in Figure 3. Here, the effluent stack was measured via representative sampling and so the plume was predicted using the national atmospheric release advisory center (NARAC) modelling code allowing comparison with offsite sampling stations [9].

2.2.1 Source of the WIPP release

The release itself was comprised of a nitric salt with around 7 curies of ^{241}Am contained therein. The cause of the deflagration was eventually traced back to the use of organic kitty litter with the nitric salt based on a miscommunication of the words, "inorganic" with "an organic". Detailed descriptions of the sequence of events culminating in the release can be found elsewhere [10].

2.2.2 Air monitoring results

A graph of the predicted versus measured air concentration values from the WIPP event is provided in Figure 4 [1, 6]. Here it is clear that at high airborne concentrations, excellent linear correlation is realized resulting in an almost unity correspondence. At lower concentrations however, a drastically larger relative deviation is clearly seen in Figure 4.

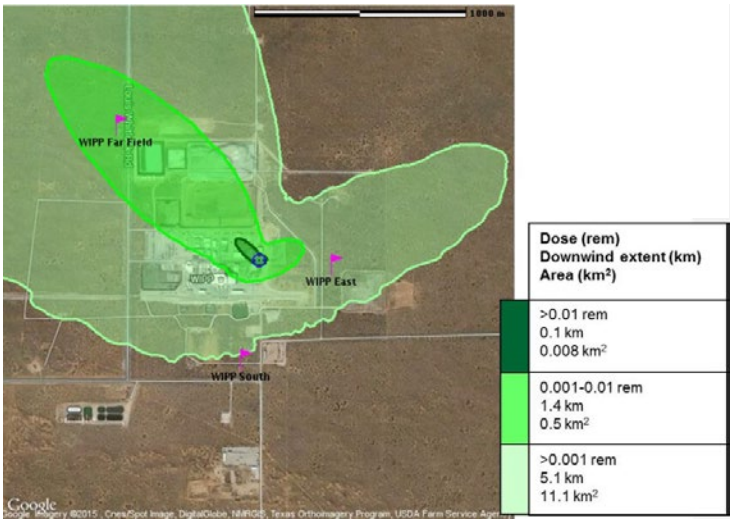

Figure 3: Dose contours determined via NARAC from the WIPP release based on effluent assays which could then be correlated with field air sampling results. Inner locations for air sampling are represented by maroon flags labelled WIPP Far Field, WIPP East and WIPP South.

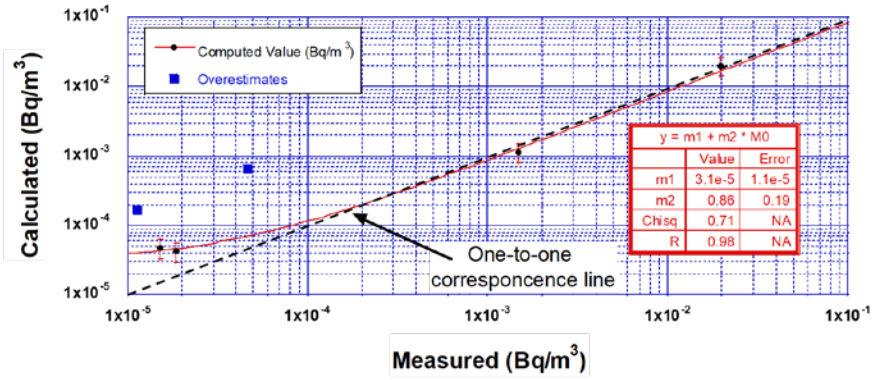

Figure 4: Plume projection predicted concentration as a function of empirical field assay values of the passing plume based on regulatory compliance air sampling infrastructure. Overestimates are also shown.

The linear correlation shown in Figure 4 does not include the pair of noted overestimates (blue squares). The agreement seen at high concentrations largely forces the high correlation. The scatter at low concentrations is noted to vary by an order of magnitude relative to the expected value with apparent presence of positive bias in overpredicting. Overpredictions will be shown later to be an expected event from small probability, large particle size radioaerosols being sampled.

3. Aerosol statistics

The shape parameter for an aerosol is based on its settling velocity in ambient air when compared to a spherical droplet of water. The equivalent water droplet with the same settling velocity as the aerosol then fixes the mass median aerodynamic diameter (MMAD). Similarly, the activity median aerodynamic diameter (AMAD) is used for defining respirable particle sizes which when inhaled can be incorporated into bodily fluids through the lung membrane of the alveoli.

An equivalence between the MMAD and AMAD can be found only when a radioaerosol has a constant specific activity. If the entire particle has uniform radioactivity present, then the activity will be directly proportional to the mass and so the reference diameter which gravitationally falls at the same rate as the standard droplets normalize them to have the same size distribution values of mode, median and mean as shown in Figure 5.

3.1 Lognormal

The functional relationship describing the shape distribution of aerosols (Fig. 5) is given by Equation 1. Here, the argument of the exponential is a logarithmic abscissa and so a typical shape for a 5 μm MMAD aerosol is shown in Figure 5. Here, the skew is evident in that the parameter describing the shape equivalent of a standard aerosol (MMAD or equivalently the AMAD) is far up into the tail and very different than the mode or median.

$$f\left(x;\mu,\sigma^2\right)=\frac{1}{\sqrt{2\pi}\sigma x}e^{-\left[\ln(x)-\mu\right]^2/\left(2\sigma^2\right)} \quad (1)$$

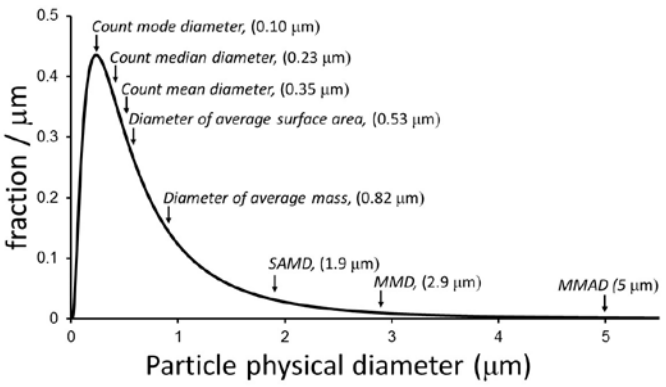

Figure 5: Probability distribution of 5 μm AMAD particles as a function of their particle physical diameter [11]. Marked in the figure are many properties of potential significance in evaluating statistical properties of a distribution from an aerosol with an AMAD of 5 μm. Other metrics shown in the figure for aerosol shape characterization are the surface aerodynamic mean diameter (SAMD) and the mass mean diameter (MMD, not the median) which use different properties of the aerosol as the weights in obtaining the average for a distribution.

The basic probability density function is approximated here by Equation 1 where more detailed physical interpretations can be obtained elsewhere [12]. An example of such a distribution is shown in Figure 5 where a frequency distribution of various diameter related metrics are provided. Here, the mode (0.1 μm) is recognized to be less than half the median (0.23 μm) which is more than an order of magnitude below the effective mean or the mass median aerodynamic diameter (MMAD at 5 μm). It is the MMAD (effectively equivalent to the activity median aerodynamic diameter or AMAD) which is standardized based on settling velocities compared to a monodisperse material such as water. This is important given the dependency on the effective shape distributions driven by conforming to Equation 1 relative to the total respirable fraction present. This can become much more complicated with multimodal distributions although these are assumed simple superpositions of multiple lognormals.

3.1.1 Health consequences

The drastic skew in particle size distributions of an aerosol (Fig. 5) can significantly affect the inhalation intake from incorporation into bodily fluids through transfer across the tissue interface of the lung alveoli. The respirable range is generally in the 0.1 to 5 μm range where most planar disc air sample filters have the largest variation in collection efficiency as seen in Figure 2.

If the shape distribution peaks (has a mode) in the respirable range where sampling efficiency demonstrates the largest variability (Figure 2), evolution in the peak location will only exacerbate the resultant health effect dispersion. This contributes to overall error but the true uncertainty has to also account for sampling statistics driven by the distributions following the form of Equation 1.

3.1.2 Sampling statistics

By definition, a small number of aerosols sampled from the diameter distribution shown in Figure 5 will likely come from the mode. On average, half of these should be above the median which itself is just over double the mode. The dispersion in diameters sampled for a small sample number would then be expected to look like a Gaussian, centered between the mode and median in this sense.

The population however has members with sufficiently large diameters which cause the aerodynamic average to be more than an order of magnitude larger than either of the erroneous Gaussian approximations to the mode or median. Based on the frequency distribution seen in Figure 5, the probability of sampling a very large diameter particle is vanishingly small. If the activity of each aerosol particle is uniform throughout its volume, then the true sampling dispersion can become egregious at best considering the effects of these very large particulates in the assay.

3.1.3 Shape parameter dependencies

The shape of the distribution seen in Figure 5 is strongly dependent on the geometrical standard deviation of the lognormal. A family of curves for the lognormal having different shape parameters are shown in Figure 6 where each curve shown has the same integrated area (note both base axes are not linear in the traditional sense as log(x) is plotted as an axis).

Here the family of curves is normalized to have the same integral to highlight the large variation possible from a lognormal distribution, specifically when they all have equivalent probability interpretations. This results in each curve having a different mode, median and mean. The curves are graphed together along the sigma scale for display only and not intended to describe the expected distribution of any specific sample as real world distributions can be multimodal and dynamic.

3.1.4 Monte Carlo modelling

A normal random variable of mean $\bar{x}$ and variance σ^2 is represented by $N\left(\bar{x},\sigma^2\right)$. A normal random variable with zero mean and unity variance is represented by the symbol $N(0,1)$. This was used to create a lognormal distribution in the form of $e^{N(0,1)}$ such that it would have a mode of e^{-1}=0.37 μm, a median of e^{0}=1 μm, and a mean of $e^{1/2}$=1.65 μm. With this mean radius, the average diameter then becomes 3.3 μm which places it in the range of the most penetrating size for biological intake and so makes for a simplified mathematical example for consideration.

A random sampling from the $e^{N(0,1)}$ distribution was done using a generated normal random variable in Microsoft Excel to allow for simulating these effects. Doing this 1E6 times resulted in the overall distribution shown in Figure 7 where the insets show the distribution's appearance when displayed with differing logarithmic axes. The upper center inset has

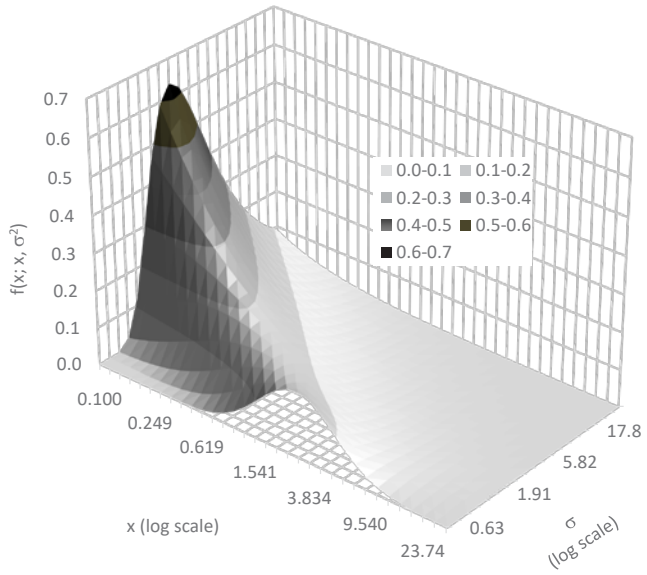

Figure 6: Family of lognormal distributions having a mean μ=1.5 μm based on a progressive increase in shape parameters as listed in the legend. Note the shape parameter is the σ value in Equation 1.

a logarithmic abscissa resulting in an apparent normal distribution. The upper right inset has a logarithmic ordinate axis showing the effect of the unique tail approximated by the Monte Carlo calculation.

Taking a random sample from a lognormal population distribution will then result in a dispersion strongly dependent on sample number. As the sample number becomes large, the true lognormal distribution will by definition be observed. Smaller sets will appear normal demonstrating skew with increasing sample size. Estimating this effect by simple Monte Carlo sampling from the population probability density function can provide a good estimate on these effects.

3.1.4.1 Normal variance as a function of sample size

Due to the choice of a simplified distribution parameter set, the normal standard deviation as a function of sample size is $\sigma(n)$ then given by the expectation function $\sigma(n)=\sqrt{\left(E\left(\bar{x}-x\right)\right)^2}$ such that when $\sigma(n)=2/\sqrt{n}$ for the particle radii distribution. This means that at the upper 95% confidence level (CL), the limit becomes $3.29/\sqrt{n}$ which relative to the defined mean (e.g. AMAD) value of $\bar{x}$ =1.65 shows that there must be at least 4 randomly sampled aerosol particulates to have a normal standard deviation of 2. This may not seem terrible at first glance but note that the activity of a transuranic or similar radioaerosol will not scale with the radii but rather the radii cubed. With low particle numbers, this activity value becomes large, effectively an order of magnitude.

A very relevant question then becomes the effect of those instances when a low probability aerosol of a large diameter is sampled from the distribution given that very large radii are possible from this very simple distribution (>20 μm, Figure 7, $e^{N(0,1)}$). Here, the activity (or mass) scales with the effective radius cubed. A singe 2.2 μm radius particle will have 10 times the activity of a single 1 μm radii particle. Likewise, a 1 μm radius particle will have 1000 times the activity of a 0.1 μm particle. More egregious cases could be considered (e.g. multimodal distributions etc.) but the salient point is that this is truly an independent dispersion source in the overall assay results.

4. Discussion

Applications of this work in treaty verification and plume monitoring demonstrate how plume density or activity measurements will have large dispersion from penumbra samples where particulate density is low or very low. Unless the aerosol itself is not homogenous in composition, this will only effect integrated activity or centerline projection estimates. The key facet in aerosol physics directs that the dispersion mechanisms do not change the average as a whole but only the variance of that mean if more common statistics (normal or Poisson) are assumed. Correspondingly, a small sample number from low concentration air will be expected to have very high dispersion as seen empirically from historical air monitoring assays when the sampled particulate number is small [13].

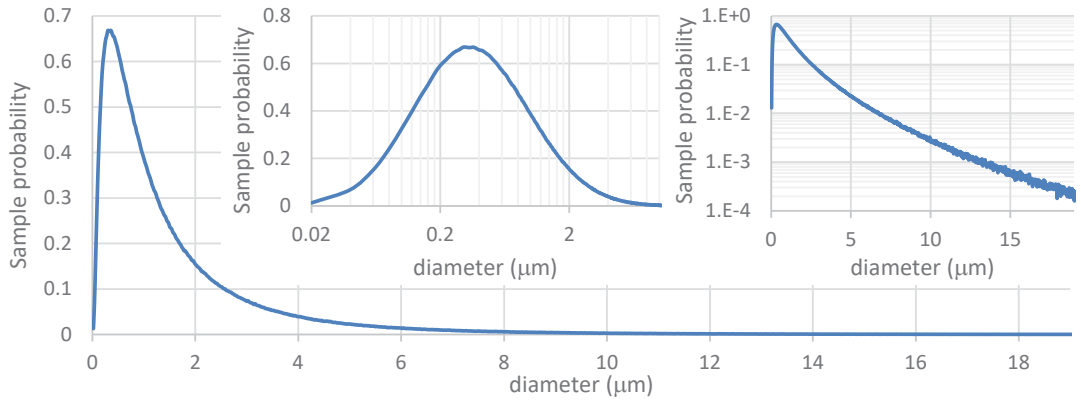

Figure 7: Monte Carlo calculated standard lognormal probability distribution from 1E6 values generated from exp(N(0,1)). This distribution has a mode at 0.34 μm, a median at 1.0 μm and a mean at 1.65 μm.

The key finding here considers that the Poisson dispersion in air filter assays may actually prove to be an insignificant contribution to the overall uncertainty in the characterization effort of any airborne contamination events. The extent to which this dispersion plays a role will be dependent on a product of the sample volume and actual airborne contamination concentration as this will scale the number of particles acquired on the filter media. Assays of high activity samples will not be subject to this additional dispersion effect to the same extent as the low activity samples and so can be considered accordingly.

The functional dependence of particle size distributions was demonstrated using a mathematically simplified distribution scaled to have relevance to radiological risk scenarios for aerosol assay. More egregious cases could be constructed as done elsewhere [6] although clearly, less egregious cases could also be constructed and considered realistic for potential real world applications in operational health physics scenarios. The moderate approach utilized here was offered as an insightful perspective into the effects from particle size distributions in final assay results and their interpretations.

5. Conclusions

This work has shown that the true dispersion in most radioaerosol samples can potentially be orders of magnitude larger than the uncertainty ascribed only from Poisson counting errors in the sample assay. Interpretations which require quantitative estimates of the radiological concentration then are subject to additional uncertainty terms which have not historically been considered when characterizing radiological air sample assay results.

6. Acknowledgements

This work partially paid through a joint faculty appointment between North Carolina State University and Oak Ridge National Laboratory in coordination with the Office of Defense Nuclear Nonproliferation R&D of the National Nuclear Security Administration sponsored Consortium for Nonproliferation Enabling Capabilities (CNEC) by the Department of Energy National Nuclear Security Administration under Award Number DE-NA0002576.

7. References

[1] Hayes RB; (2016) Consequence assessment of the WIPP radiological release from February 2014. *Health Phys.* **110**(4), 342-360.

[2] Frank-Supka L, Harward DJ, Casey SC; *Overview of the WIPP Effluent Monitoring Program, Compliance with Title 40 CFR Part 191, Subpart A, Environmental Standards for Management and Storage* US Department of Energy, Carlsbad New Mexico, May 2005. Last accessed 4/19/2019 https://wipp.energy.gov/library/Overview_WIPPEffluentMonitoring.pdf

[3] Maiello ML, Hoover MD Editors; *Radioactive Air Sampling Methods*, CRC Press, Boca Raton, FL, 2011.

[4] Kleinstreuer C, Feng Y. Computational Analysis of Non-Spherical Particle Transport and Deposition in Shear Flow With Application to Lung Aerosol Dynamics—A Review. *ASME. J Biomech Eng.* 2013;**135**(2):021008-021008-19. doi:10.1115/1.4023236

[5] Vehkamäki H, Riipinen I, Stockholms universitet, Naturvetenskapliga fakulteten, Institutionen för tillämpad miljövetenskap (ITM). Thermodynamics and kinetics of atmospheric aerosol particle formation and growth. *Chemical Society reviews*. 2012;**41**:516-5173.

[6] Hayes RB. (2017) Reconstruction of a radiological release using aerosol sampling *Health Phys*. **112**(4), 326-337.

[7] Hendricks T, Hayes R. Enhancement of aerial gamma surveillance utilizing complementary characteristics of NaI and HPGe detection. *1st Joint Emergency Preparedness and Response/Robotic and Remote Systems Topical Meeting*. Salt Lake City, UT, February 11-16, 2006. ISBN: 978-0-89448-692-0 CD-ROM.

[8] Hayes RB, Akbarzadeh M. (2014) Using isotopic ratios for discrimination of environmental anthropogenic radioactivity. *Health Phys.* **107**, 277-291.

[9] Hayes RB. (2016) Consequence assessment of the WIPP radiological release from February 2014. *Health Phys.* **110**(4), 342-360.

[10] Accident Investigation Board. *Radiological Release Event at the Waste Isolation Pilot Plant, February 14, 2014*. US Department of Energy, Carlsbad, New Mexico. April 2015. Accessed 4/20/19 https://www.wipp.energy.gov/Special/AIB_WIPP%20Rad_Event%20Report_Phase%20II.pdf

[11] Hoover MD. SC 2.6: *Radiation Safety Aspects of Nanotechnology*. National Council on Radiation Protection and Measurements, Bethesda MD 2016

[12] Crow EL, Kunio Shimizu K, Editors; *Lognormal distributions: theory and applications.* Taylor and Francis, London, 2017

[13] Alvarez JL, Bennett WS, Davidson TL; Design of an Airborne Plutonium Survey Program for Personnel Protection. *Health Physics.* **66**(6):634-642, June 1994.